Neurobiology:

α-SNAP Interferes with the Zippering of the SNARE Protein Membrane Fusion Machinery

Yongsoo Park, Wensi Vennekate, Halenur Yavuz, Julia Preobraschenski, Javier M. Hernandez, Dietmar Riedel, Peter Jomo Walla and Reinhard Jahn

J. Biol. Chem. 2014, 289:16326-16335.
doi: 10.1074/jbc.M114.556803 originally published online April 28, 2014

THE JOURNAL OF BIOLOGICAL CHEMISTRY VOL. 289, NO. 23, pp. 16326–16335, June 6, 2014

α-SNAP Interferes with the Zippering of the SNARE Protein Membrane Fusion Machinery

Received for publication, February 11, 2014, and in revised form, April 25, 2014 Published, JBC Papers in Press, April 28, 2014, DOI 10.1074/jbc.M114.556803

Yongsoo Park[‡], **Wensi Vennekate**[‡§], **Halenur Yavuz**[‡], **Julia Preobraschenski**[‡], **Javier M. Hernandez**[‡1], **Dietmar Riedel**[¶], **Peter Jomo Walla**[§‖], **and Reinhard Jahn**[‡2]

From the [‡]*Department of Neurobiology, the* [§]*AG Biomolecular Spectroscopy and Single-Molecule Detection, and the* [¶]*Facility for Electron Microscopy, Max-Planck-Institute for Biophysical Chemistry, 37077 Göttingen and the* [‖]*Department of Biophysical Chemistry, Institute for Physical and Theoretical Chemistry, Technical University of Braunschweig, 38106 Braunschweig, Germany*

Background: Soluble *N*-ethylmaleimide-sensitive factor attachment protein α (α-SNAP) regulates the pre-fusion step as well as SNARE disassembly.
Results: α-SNAP on its own interferes with SNARE zippering and inhibits chromaffin granule fusion, but not synaptic vesicle fusion.
Conclusion: Retardation of SNARE zippering by α-SNAP results in the partial SNARE zippering.
Significance: This is the first direct evidence showing the partial SNARE zippering in the physiological context.

Neuronal exocytosis is mediated by soluble *N*-ethylmaleimide-sensitive factor attachment protein receptor (SNARE) proteins. Before fusion, SNARE proteins form complexes bridging the membrane followed by assembly toward the C-terminal membrane anchors, thus initiating membrane fusion. After fusion, the SNARE complex is disassembled by the AAA-ATPase *N*-ethylmaleimide-sensitive factor that requires the cofactor α-SNAP to first bind to the assembled SNARE complex. Using chromaffin granules and liposomes we now show that α-SNAP on its own interferes with the zippering of membrane-anchored SNARE complexes midway through the zippering reaction, arresting SNAREs in a partially assembled *trans*-complex and preventing fusion. Intriguingly, the interference does not result in an inhibitory effect on synaptic vesicles, suggesting that membrane properties also influence the final outcome of α-SNAP interference with SNARE zippering. We suggest that binding of α-SNAP to the SNARE complex affects the ability of the SNARE complex to harness energy or transmit force to the membrane.

Neurotransmitters are stored in synaptic vesicles and secretory granules and are released by Ca^{2+}-dependent exocytosis upon stimulation. Fusion between vesicles and the plasma membrane are mediated by soluble *N*-ethylmaleimide-sensitive factor attachment protein receptor (SNARE) proteins. These include the transmembrane synaptobrevin-2 residing in the vesicle membrane, and SNAP[3]-25A and syntaxin-1A residing in the plasma membrane (1, 2). SNARE proteins are characterized by a conserved heptad repeat of 60–70 residues known as SNARE motifs, which assemble into a four-helix bundle consisting of 16 layers of interacting amino acids called the SNARE complex (1). Both synaptobrevin-2 and syntaxin-1A possess a single SNARE motif connected by a short linker to a C-terminal transmembrane domain, whereas SNAP-25 possesses two SNARE motifs connected by a flexible linker that is palmitoylated and anchored to the membrane (1).

According to the zipper hypothesis, membrane fusion is mediated by the highly exergonic assembly of the SNARE motifs into a four-helix bundle that bridges the membranes (*trans*-configuration). In exocytosis of synaptic vesicles, assembly of the bundle appears to be preceded by the formation of a transient syntaxin·SNAP-25 binary complex, which contains an acceptor site for synaptobrevin-2 (1, 3). Once the acceptor complex is formed, assembly is initiated at the membrane-distal ends and then progresses toward the C-terminal membrane anchors, thereby bringing the vesicle and plasma membrane into close proximity (4, 5) and overcoming the repulsion between the membranes (6). Once complete in this *cis*-configuration, the SNARE complex is disassembled by the AAA^{+} ATPase NSF (*N*-ethylmaleimide-sensitive factor) (7). NSF-driven disassembly requires a cofactor termed SNAP (acronym for soluble NSF attachment protein, the dominant isoform being α-SNAP (8, 9)), which first binds to the SNARE complex and then recruits NSF, catalyzing its disassembly in an ATP-dependent manner (8). It has been demonstrated that α-SNAP binds to SNARE complexes in an antiparallel manner (10–12). Furthermore, a hydrophobic loop at the N terminus binds to phospholipid bilayers and enhances the binding affinity of α-SNAP to membrane-embedded SNARE complexes (13). Intriguingly, α-SNAP also binds to the syntaxin·SNAP-25 binary acceptor complex and even to free syntaxin, resulting in

[1] Present address: Dept. of Cellular and Molecular Biophysics, Max-Planck-Institute for Biochemistry, Am Klopferspitz 18, 82152 Martinsried, Germany.
[2] To whom correspondence should be addressed: Am Fassberg 11, 37077 Göttingen, Germany. Tel.: 49-551-201-1635; Fax: 49-551-201-1499; E-mail: rjahn@gwdg.de.
[3] The abbreviations used are: SNAP, soluble *N*-ethylmaleimide-sensitive factor attachment protein; NSF, *N*-ethylmaleimide-sensitive factor; CG, chromaffin granule; PE, L-α-phosphatidylethanolamine; NBD-DOPE, 1,2-dioleoyl-*sn*-glycero-3-phosphoethanolamine-*N*-(7-nitrobenz-2-oxa-1,3-diazol-4-yl; rhodamine-DOPE, 1,2-dioleoyl-*sn*-glycero-3-phosphoethanolamine-*N*-lissamine rhodamine B sulfonyl ammonium salt; FCCS, fluorescence cross-correlation spectroscopy; SV, synaptic vesicle; FCS, fluorescence correlation spectroscopy; TeNT, tetanus toxin.

the recruitment of NSF, and ATP-dependent dissociation (11, 14, 15). However, the physiological significance of these interactions remains unclear.

Although the presumed role of α-SNAP is confined to disassembly and thus to re-generation of SNAREs, a few studies have reported that α-SNAP on its own can inhibit exocytosis of large vesicles in *Drosophila* (16), sperm acrosome fusion (17, l8), yeast vacuole fusion (19, 20), and dense-core vesicle exocytosis in PC12 cells (21). The molecular mechanisms by which α-SNAP inhibits fusion of these vesicles are unclear, but it is known that this inhibition is prevented in the presence of NSF. In the yeast vacuole system, Sec17p, the yeast ortholog of α-SNAP, inhibits fusion, whereas SNAREs are still capable of engaging in *trans* (22), suggesting it may act on a late step in the fusion pathway.

In the present study, we use *in vitro* docking and fusion assays involving purified chromaffin granules (CGs) and liposomes to show that binding of α-SNAP to the SNARE complex can be inhibitory to fusion. More specifically, our data suggests that α-SNAP slows down and interferes with SNARE zippering in the middle portion of the SNARE bundle, an effect that probably reduces force transmission and the harnessing of the energy released and utilized by the SNARE complex for membrane fusion.

EXPERIMENTAL PROCEDURES

Materials—2Na-ATP was purchased from AppliChem (Darmstadt, Germany). Antibodies to synaptobrevin-2 (clone number 69.1) and α-SNAP (clone number 77.1) were from Synaptic Systems (Göttingen, Germany). Alexa Fluor 488 C5 maleimide, Texas Red C5 bromoacetamide, and Oregon Green 488 iodoacetamide were from Invitrogen.

Purification of CGs and Synaptic Vesicles—CGs were purified from bovine adrenal medullae using continuous sucrose gradient centrifugation as described before (23) and resuspended in 120 mM potassium glutamate, 20 mM potassium acetate, 20 mM HEPES-KOH, pH 7.4. Synaptic vesicles from rat brain were purified as described in detail elsewhere (24).

Protein Purification—All SNARE and complexin II constructs were based on rat sequences, expressed in *Escherichia coli* strain BL21(DE3) and purified by Ni^{2+}-NTA affinity chromatography followed by ion-exchange chromatography. The stabilized Q-SNARE acceptor complex (ΔN complex) consisting of syntaxin-1A (amino acids 183–288), SNAP-25A (no cysteine, cysteines were replaced by alanines), and the C-terminal synaptobrevin-2 fragment (amino acids 49–96) and the soluble stabilized Q-SNARE complex with syntaxin-1A(183–262) were purified as described earlier (4). The Q-SNARE complex containing full-length syntaxin-1A(1–288) and SNAP-25A (no cysteine, cysteines were replaced by alanines) was expressed using co-transformation (25). The stabilized Q-SNARE complex and Q-SNARE complex (full-length syntaxin-1A·SNAP-25A) were purified by ion-exchange chromatography on an MonoQ column (GE Healthcare) in the presence of 50 mM *n*-octyl-β-D-glucoside. Full-length synaptobrevin-2, soluble synaptobrevin-2 lacking the transmembrane domain (Syb(1–96)), and C2AB domain of synaptotagmin-1(97–421) were purified by MonoS column. Chinese hamster NSF, bovine α-SNAP wild-type, and mutants including α-SNAP (F27S, F28S) and α-SNAP(33–295) were expressed and purified as described in detail elsewhere (13).

For anisotropy measurements, syntaxin-1A (Cys^{225}) of the soluble stabilized Q-SNARE complex or Syb(49–96) (Cys^{79}) in the stabilized Q-SNARE complex were labeled with Alexa Fluor 488 C5 maleimide (13). For FRET measurement to monitor SNARE assembly, single cysteine mutations of SNAP-25A (Cys^{130}) and Syb(1–96) (Cys^{28}) were labeled with Texas Red C5 bromoacetamide and Oregon Green 488 iodoacetamide, respectively.

Preparation of Proteoliposomes—Lipid composition of proteoliposomes containing the Q-SNARE complex consists of 45% L-α-phosphatidylcholine), 15% PE (L-α-phosphatidylethanolamine), 10% L-α-phosphatidylserine, 25% cholesterol, 4% L-α-phosphatidylinositol, and 1% phosphatidylinositol-(4,5)P_2. For FRET-based dequenching assays, 1.5% 1,2-dioleoyl-*sn*-glycero-3-phosphoethanolamine-*N*-(7-nitrobenz-2-oxa-1, 3-diazol-4-yl (NBD-DOPE) and 1.5% 1,2-dioleoyl-*sn*-glycero-3-phosphoethanolamine-*N*-lissamine rhodamine B sulfonyl ammonium salt (Rhodamine-DOPE) were replaced as a donor and an acceptor dye, respectively (26). Synaptobrevin-2-containing liposomes consist of 55% L-α-phosphatidylcholine, 20% PE, 15% L-α-phosphatidylserine, and 10% cholesterol. For measurement of fluorescence cross-correlation spectroscopy (FCCS) in Fig. 4, *b* and *c*, 1.5% NBD-DOPE and rhodamine-DOPE were included in synaptobrevin-2- and the Q-SNARE complex-containing liposomes, respectively. 15% PE (without labeled-PE) was used for measurement of FRET and anisotropy. All lipids were from Avanti Polar Lipids.

Incorporation of SNARE proteins into large unilamellar vesicles was achieved by *n*-octyl-β-D-glucoside-mediated reconstitution with a protein to lipid molar ratio of 1:500, as described (26). Proteoliposomes containing the Q-SNARE complex or synaptobrevin-2 were prepared using insertion into large unilamellar vesicles by reverse phase evaporation and extrusion through polycarbonate membranes with 100-nm pore size (23, 26). Polycarbonate membranes with different pore sizes were used to produce liposomes in different sizes, and liposome size was analyzed using FCS (data not shown).

Fusion Reaction—CG fusion reactions were performed at 37 °C. For each reaction, CGs and proteoliposomes were mixed in 1 ml of buffer containing 120 mM potassium glutamate, 20 mM potassium acetate, 20 mM HEPES-KOH, pH 7.4, and 5 mM $MgCl_2$. 5 mM 2Na-ATP was added to activate NSF as indicated specifically. Fluorescence dequenching was measured using a Fluoromax (Horiba Jobin Yvon) with wavelengths of 460 nm (slit width of 1 nm) for excitation and 538 nm (slit width of 3 nm) for emission. De-quenching of the donor fluorescence was normalized as the percentage value of the maximum donor fluorescence induced by 0.1% Triton X-100 detergent treatment at the end of experiments. No addition represents basal fusion without any treatment.

Fluorescence Anisotropy Measurements—Anisotropy measurements were carried out in a Fluorolog 3 spectrometer in T-configuration equipped for polarization (model FL322, Jobin Yvon). Unless stated otherwise, all experiments were performed at 37 °C in 1 ml of buffer containing 120 mM potassium

glutamate, 20 mM potassium acetate, 20 mM HEPES-KOH, pH 7.4, and 5 mM $MgCl_2$. 5 mM 2Na-ATP was added for SNARE disassembly experiments to activate NSF. Excitation wavelength was 488 nm with slit width of 8 nm and emission was measured at 520 nm with slit width of 10 nm. CGs or synaptic vesicles (SV) were incubated with liposomes incorporating the stabilized Q-SNARE complex in which Syb(49–96) was labeled with Alexa Fluor 488 C5 maleimide at Cys^{79}. Soluble unlabeled synaptobrevin-2 (Syb(1–96)) was applied for the complete dissociation of labeled Syb(49–96). In case of the soluble stabilized Q-SNARE complex, 40 nM of the soluble stabilized complex (syntaxin-1A labeled with Alexa Fluor 488 C5 maleimide at Cys^{225}) was incubated with CGs. Anisotropy was presented as A/A_0, where A_0 is the initial value. In Fig. 5, *d* and *e*, anisotropy was normalized by scaling the initial and final value as 1 and 0, respectively.

Fluorescence Resonance Energy Transfer (FRET)—SNAP-25A (Cys^{130}) in the stabilized Q-SNARE complex was labeled with Texas Red C5 bromoacetamide and Syb(1–96) (Cys^{28}) was labeled and Oregon Green 488 iodoacetamide. SNARE assembly led to quenching of donor fluorescence. Oregon Green 488 donor fluorescence was measured using a Fluoromax (Horiba Jobin Yvon) with excitation and emission wavelengths for 488 and 520 nm, respectively. Fluorescence intensity was presented as F/F_0, where F_0 is the initial value.

Fluorescence Correlation Spectroscopy (FCS)—As described before (27), a titanium-sapphire laser (800 nm, 87 MHz) for two-photon excitation was coupled to an Axiomat inverse microscope (Zeiss, Germany). The diffusion time characterizes the average residence time that a rhodamine-labeled liposome needs to diffuse through the focal volume of about 0.3 fl and width of 200 nm. The size distribution of proteoliposomes (100 and 200 nm in diameter) was determined by calculating the diffusion time (data not shown). The diffusion time of proteoliposomes increases linearly with the diameter of liposomes (28).

FCCS was performed to measure docking of liposomes, as described in detail elsewhere (27). FCCS discriminates free or docked liposomes as liposomes pass through the focal volume of a dual detection fluorescence confocal set-up. NBD- and rhodamine-labeled phospholipids are incorporated in synaptobrevin-2-liposomes and the Q-SNARE complex liposomes, respectively. Simultaneous dual detection of fluorescence bursts observed in the focal volume corresponds either to fusion or docking of liposomes, the signals of which are then said to be cross-correlated. Fusion can be further distinguished from docking by measuring changes in the fluorescence lifetime of the donor dye as a result of FRET after lipid mixing (26, 27).

Determination of Tetanus Toxin-resistant SNARE Complexes—The light chain of TeNT is a Zn^{2+}-protease that selectively degrades free synaptobrevin-2, whereas synaptobrevin-2, partially or fully assembled in the ternary SNARE complex, is resistant to cleavage (29). Incubation of CGs with liposomes containing the stabilized Q-SNARE complex for 10 min at 37 °C led to the formation of the ternary SNARE complex. Ternary SNARE complex was disrupted by boiling and TeNT-resistant synaptobrevin-2 represented partial or full SNARE assembly (Fig. 3*d*).

Liposome Co-flotation Assay—200 nm Synaptobrevine-2-liposomes were incubated with liposomes containing the stabilized Q-SNARE complex (Syb(49–96) labeled with Alexa Fluor 488) in the presence of 500 nM α-SNAP for 30 min at 37 °C. The samples were then mixed with Nycodenz (Axis Shield, 80%, 30 μl) and a second Nycodenz layer (30%, 50 μl) was gently applied followed by another layer of buffer (40 μl). The density gradient was centrifuged with a Beckman TL-100 ultracentrifuge (TLS55 rotor, 100,000 × *g*, 4 °C, 1 h). 25-μl Aliquots were carefully taken from the top of the gradient and analyzed in fluorescence intensity.

Cryoelectron Microscopy—As described previously (23), liposomes were imaged with a CM 120 transmission electron microscope and pictures were taken with a TemCam 224A slow scan CCD camera (TVIPS, Gauting, Germany). 200 nm Synaptobrevin-2-liposomes were incubated with 100-nm liposomes containing the stabilized Q-SNARE complex in the presence or absence of 500 nM α-SNAP for 1 h at 37 °C. Liposomes were classified as undocked (single liposome), docked (one contact by two liposomes), and clustered (multiple docking by more than three liposomes) and quantified as percentage of total number of liposomes.

Statistical Analysis—All quantitative data are mean ± S.D. or S.E. Dose-response curves were fitted using four parameter logistic equations (4PL) to calculate IC_{50} (SigmaPlot).

RESULTS

α-SNAP Inhibits SNARE-mediated Fusion of CGs—We have shown previously that purified CGs (approximately 200 nm in average diameter) readily fuse with liposomes containing the syntaxin·SNAP-25 acceptor complex in a SNARE-dependent manner involving endogenous synaptobrevin-2 (23). Preincubation of acceptor liposomes (approximately 100 nm diameter (26)) with recombinant α-SNAP (500 nM, 5 min at 37 °C) resulted in a strong inhibition of fusion (Fig. 1, *a–c*), regardless of whether the acceptor liposomes contained full-length syntaxin-1A and SNAP-25A (henceforth Q-SNARE complex) (Fig. 1*a*) or a truncated complex stabilized by a C-terminal fragment of synaptobrevin-2 (Syb(49–96), termed the stabilized Q-SNARE complex) (Fig. 1*b*). The latter was shown previously to result in markedly enhanced fusion rates due to the availability of a free binding site for synaptobrevin-2, with the stabilizing peptide being displaced during the fusion reaction (4). In this complex we also determined the efficacy (measured as apparent IC_{50}) of α-SNAP inhibition to be 219 ± 25 nM (Fig. 1*c*). Note that NSF does not inhibit fusion considerably in the absence of α-SNAP (Fig. 1*a*).

Under physiological conditions, α-SNAP binding to the SNARE complex results in the recruitment of NSF, which leads to disassembly of the complex. Indeed, the inhibitory action of α-SNAP on exocytosis observed previously was rescued by NSF (16–21). We therefore investigated whether NSF was capable of reverting the inhibition on fusion *in vitro*. In the absence of ATP, NSF and α-SNAP again resulted in a strong inhibition (Fig. 1*d*), however, fusion was restored in the presence of ATP (Fig. 1*d*), correlating with *in vivo* data (16–21).

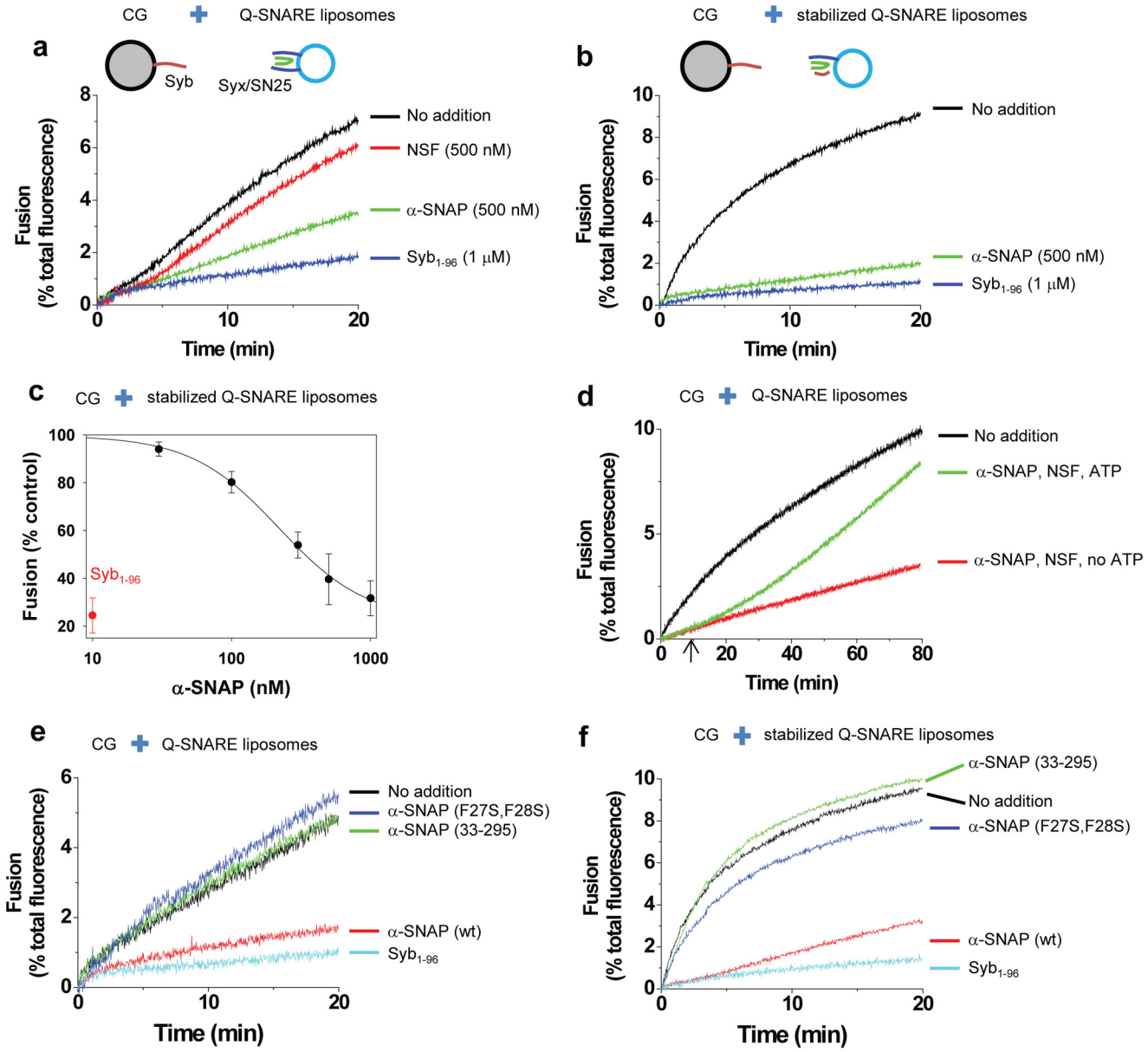

FIGURE 1. **α-SNAP inhibits SNARE-mediated fusion of CG with liposomes.** Fusion was monitored using a lipid-mixing assay based on fluorescence dequenching. Acceptor liposomes incorporated either a preformed complex containing full-length syntaxin-1A and SNAP-25A (Syx/SN25, Q-SNARE complex) (*a*) or a stabilized Q-SNARE complex containing N terminally truncated syntaxin-1A, SNAP-25A, and a C-terminal fragment of synaptobrevin-2 (stabilized Q-SNARE complex (4)) (*b*). *No addition*, basal fusion without additional proteins. The soluble fragment of synaptobrevin-2 (*Syb*(*1–96*)) was used as a competitive inhibitor for the endogenous synaptobrevin-2 in CGs, resulting in effective inhibition of fusion. *c*, a dose-response analysis of fusion inhibited by α-SNAP revealed an IC_{50} of 219 ± 25 nM. Data are mean ± S.D. from 3–5 independent experiments. *d*, when acceptor liposomes are incubated with both NSF and α-SNAP, fusion was inhibited in the absence of ATP but rescued when 100 nM NSF and 5 mM ATP were added 10 min after the reaction was started (*arrow*). 10 μM SNAP-25A was preincubated to facilitate SNARE re-assembly. *e* and *f*, α-SNAP mutants impairing the N-terminal hydrophobic loop, α-SNAP (F27S, F28S) and α-SNAP(33–295), were ineffective of preventing the fusion process, regardless of whether full-length Q-SNAREs (*e*) or stabilized Q-SNARE complexes were used (*f*).

It was shown previously that efficient binding of α-SNAP to membrane-anchored SNAREs requires a hydrophobic loop region (residues 27–32) (13), which serves as a membrane attachment site and increases the affinity of α-SNAP to the SNARE complex. To evaluate whether simultaneous binding of α-SNAP to the SNARE complex and the membrane are required for inhibiting fusion, we took advantage of two α-SNAP mutants that were previously shown to inactivate the hydrophobic loop (13). In the first mutant, two adjacent phenylalanine residues are substituted by serine (F27S, F28S), and in the second the entire N-terminal loop is deleted (33–295). As shown in Fig. 1, *e* and *f*, addition of both α-SNAP mutants at a concentration where α-SNAP (WT) approaches maximal inhibition (1 μM) did not result in an inhibition of fusion regardless of whether full-length Q-SNAREs or the stabilized Q-SNARE acceptor complex were used, supporting the view that the hydrophobic loop of α-SNAP is required for inhibition of CG fusion.

Fusion Inhibition by α-SNAP Occurs at a Step after SNARE-mediated Docking—In the next experiments, we investigated in more detail at which step in the fusion pathway the inhibition is exerted. In particular, we asked whether SNARE-dependent vesicle docking occurs in the presence of α-SNAP. To this end,

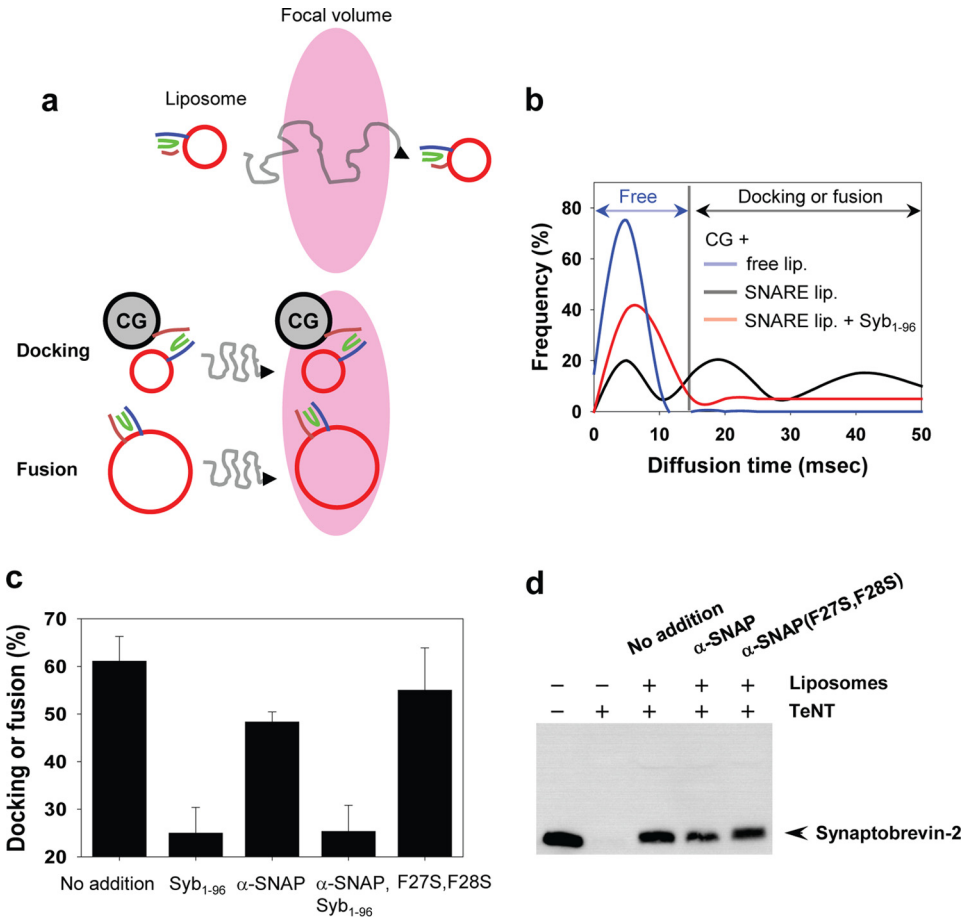

FIGURE 2. **α-SNAP inhibits CG fusion but not CG docking.** *a,* diffusion time of Q-SNARE liposomes labeled with rhodamine-phosphatidylethanolamine was measured by FCS. In this method, particles diffusing through a confocal spot of 0.3 fl are monitored and the diffusion time, the average residence time of a rhodamine-labeled liposome in the focal volume, is determined. Because the diffusion time scales with the size of the labeled particle (28), the diffusion time is increased when a labeled liposome is docked or fused with unlabeled and larger CGs. *b,* diffusion time distribution of liposomes that either do not contain proteins or contain the stabilized Q-SNARE complex. The diffusion time of liposomes was determined after 5 min of incubation with CGs and 15 ms was applied as the upper limit for discriminating free liposomes from docked or fused liposomes. Frequency of liposomes ($n = 30$) was presented with a histogram according to the diffusion time of liposomes. *c,* liposomes, docked or fused with CGs, were presented as percentage of total liposomes ($n = 30$). *No addition,* incubation of the Q-SNARE-containing liposomes with CGs without any treatment. Data are mean ± S.E. from 5 independent experiments. Syb(1–96), 1 μM; α-SNAP and α-SNAP (F27S, F28S), 500 nM. *d,* SNARE complexes form in the presence of α-SNAP although fusion is largely inhibited. A fusion reaction between CGs and liposomes containing the stabilized Q-SNAREs was allowed to proceed for 10 min, followed by the addition of the TeNT light chain, which is known to cleave only free synaptobrevin-2 (29). When fusion is allowed to proceed (no addition), the majority of endogenous synaptobrevin-2 becomes toxin-resistant, in contrast to free CGs where synaptobrevin-2 is completely cleaved.

we used FCS to monitor the diffusion time of acceptor liposomes labeled with the fluorescence dye rhodamine. Both docking and fusion of the labeled liposomes with CGs is expected to increase diffusion time due to an increase in size (28). To test this, we carried out a standard fusion reaction between purified CGs and labeled acceptor liposomes containing the stabilized Q-SNARE complex (*i.e.* similar to that shown in Fig. 1*b*). Five min after mixing, an aliquot was removed and immediately analyzed by FCS. A major increase in the diffusion time was observed as liposome passed through the focal volume (Fig. 2). The increase was completely prevented by preincubation with soluble synaptobrevin-2 (Syb(1–96), Fig. 2, *b* and *c*), indicating that the increase of the diffusion time of liposomes requires SNARE assembly in *trans*. In the presence of α-SNAP an increase in diffusion time was still detected (Fig. 2*c*) even though fusion was largely inhibited (Fig. 1*b*), indicating liposomes and CGs are predominantly in a docked state. In accordance with fusion measurements (Fig. 1, *e* and *f*), no inhibition was observed when the inactive α-SNAP mutant (F27S, F28S) was used (Fig. 2*c*).

To determine the state of SNARE assembly during incubation with α-SNAP, we then added the light chain of tetanus toxin (TeNT), a protease specific for synaptobrevin-2, at the end of the reaction. Assembled SNARE complexes are resistant to cleavage, whereas free synaptobrevin-2 is exposed to proteolytic cleavage, thus allowing for the use of the toxin to monitor SNARE complex formation (29). As shown in Fig. 2*d*, synaptobrevin-2 in free CGs was degraded by TeNT, whereas it was largely toxin resistant after fusion, indicating formation of SNARE complexes. Intriguingly, a sizeable fraction of synaptobrevin-2 (albeit smaller than that observed after fusion) also became toxin-resistant despite the fact that fusion was completely inhibited by α-SNAP, suggesting that some SNAREs were assembled and probably remained kinetically trapped in *trans* complexes. In line with the rest of our characterization, the α-SNAP mutant (F27S, F28S) had no effect as the amount of

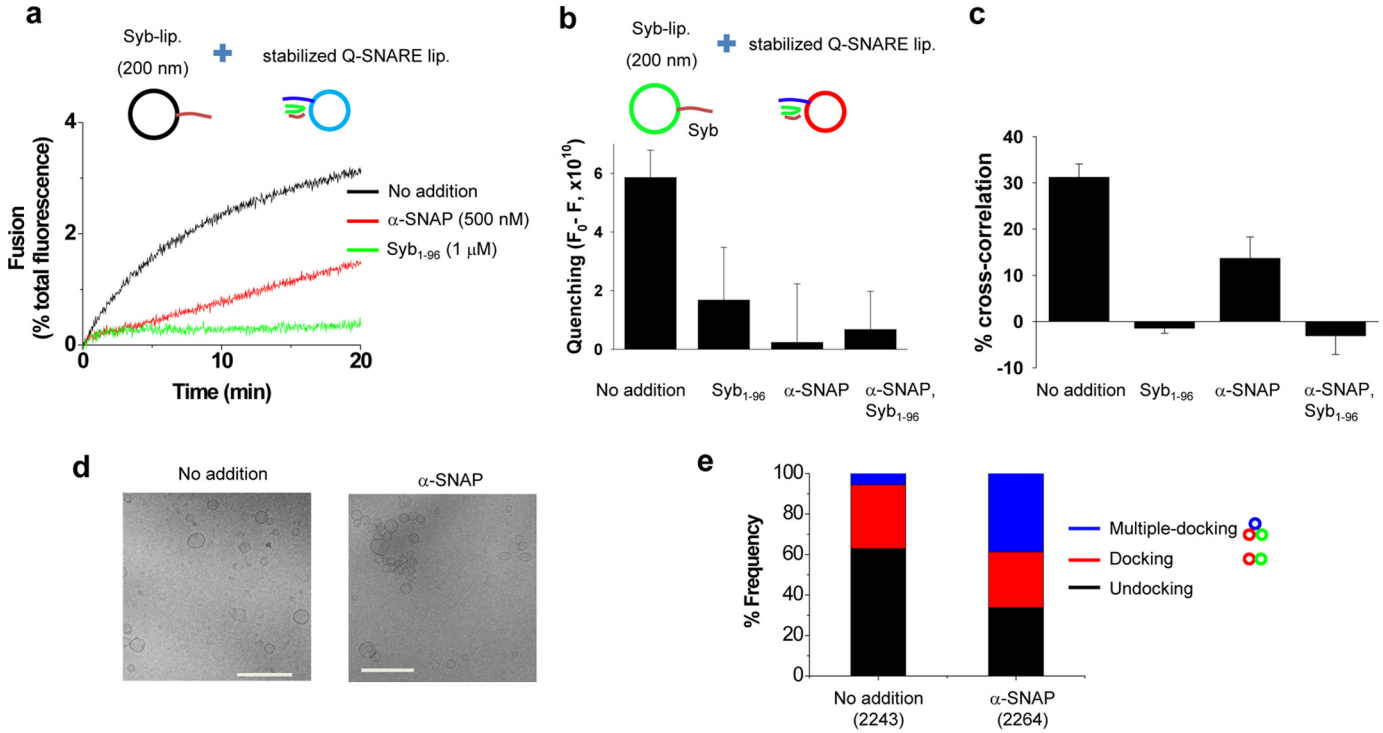

FIGURE 3. **α-SNAP inhibits SNARE-mediated fusion of liposomes.** *a,* fusion of synaptobrevin-2-containing liposomes with acceptor liposomes containing the stabilized Q-SNAREs was monitored by a standard fluorescence dequenching assay (see Fig. 1). *b* and *c*, FCCS was carried out to discriminate between docking and fusion (see "Experimental Procedures" for details). FCCS analysis was carried out 5 min after the start of the reaction, *i.e.* a time point at which fusion was not yet measurable. In the presence of α-SNAP, fusion was completely inhibited as monitored by a decrease in donor quenching (*b*), in agreement with the bulk assay shown in *panel a*. Quenching of the donor fluorescence intensity was presented as $F_0 - F$, where F_0 is the initial value. In contrast, significant cross-correlation was observable in the presence of α-SNAP indicative of docking, which was inhibited upon preincubation with Syb(1–96) (*c*). Data are mean ± S.E. (30 samples from one experiment). *d* and *e*, cryoelectron microscopy was performed to confirm liposome docking by α-SNAP. Synaptobrevin-2-containing 200-nm liposomes were incubated with 100-nm liposomes containing the stabilized Q-SNARE complex in the absence and presence of 500 nM α-SNAP. *Scale bar*, 500 nm. *e,* images were analyzed by counting free and clustered vesicles, with the clusters further being differentiated into clusters containing two or multiple vesicles (given as percent of total counted particle number, number of counted vesicles indicated in *parentheses*).

toxin-resistant synaptobrevin-2 was comparable with the uninhibited fusion reaction (Fig. 2*d*).

α-SNAP Action on Synaptobrevin-2-Liposomes Exhibit Similar Characteristics to CGs—We next asked whether the inhibitory action of α-SNAP observed after the initiation of SNARE-mediated docking on CGs could be reproduced *in vitro* with liposomes. For this we prepared synaptobrevin-2-containing liposomes with an approximate diameter of 200 nm, which were incubated with acceptor liposomes of 100 nm. Fusion was largely inhibited to a similar extent with CGs (Fig. 3*a*). To exclude that this inhibition was a result of reduced docking, we performed FCCS analysis to discriminate docking from fusion using sets of liposomes labeled with NBD-phosphatidylethanolamine (donor) and rhodamine-phosphatidylethanolamine (acceptor) (27). When 200 nm synaptobrevin-2-liposomes were analyzed 5 min after initiation of the reaction, substantial fluorescence cross-correlation was detected in the presence of α-SNAP without changing fluorescence lifetime of the donor dye (Fig. 3, *b* and *c*), indicating docking in the absence of fusion. This was confirmed by cryo-electron microscopy (EM) showing that the frequency of multiply docked liposomes increased when α-SNAP was present (Fig. 3, *d* and *e*). Together these experiments demonstrate the inhibitory effect of α-SNAP on synaptobrevin-2, liposomes occurs at a step after the establishment of the SNARE-mediated docking as was the case for CGs.

α-SNAP Interferes with SNARE Zippering via the Hydrophobic Loop—The data thus far can be explained either by α-SNAP interfering with SNARE zippering and/or by inhibiting membrane contact, *e.g.* by steric hindrance. To test whether α-SNAP is capable of interfering with zippering during SNARE complex assembly on membranes, we used a FRET-based assay to monitor the assembly of soluble synaptobrevin-2 (Oregon Green-labeled) with a stabilized Q-SNARE complex containing a Texas Red-labeled SNAP-25A. Using quenching of the donor as a reporter for SNARE assembly (30), we observed that α-SNAP slowed down assembly kinetics in a dose-dependent manner, suggesting that α-SNAP interferes with SNARE complex formation (Fig. 4*a*). Next, based on our observation that the α-SNAP mutant impairing membrane attachment failed to inhibit fusion (Fig. 1, *e* and *f*), we further tested whether membrane attachment of α-SNAP is essential for retardation of SNARE assembly. We found that membrane-free SNARE complex assembly carried out in solution was only weakly blocked by α-SNAP (Fig. 4*b*), a finding also observed with the membrane-impaired α-SNAP (F27S, F28S) mutant when the Q-SNARE was reconstituted on a liposome (Fig. 4*c*). These results suggest that zippering interference requires membrane binding as an integral part of the mechanism of fusion inhibition by α-SNAP.

An alternative way of monitoring SNARE assembly is by measuring displacement of the Syb(49–96) fragment from the

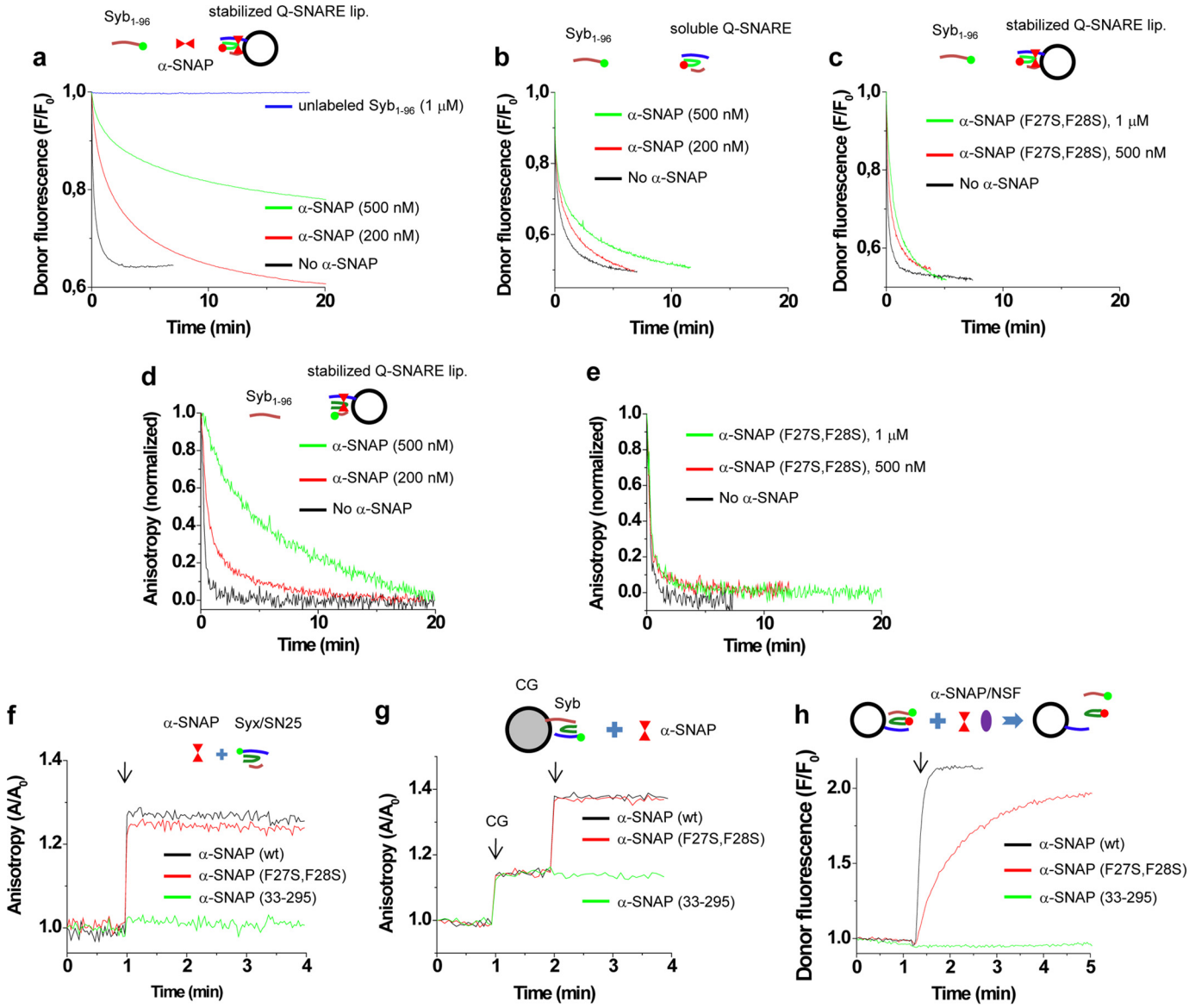

FIGURE 4. **α-SNAP interferes with SNARE assembly.** *a*, SNARE assembly was monitored using FRET in which soluble Syb(1–96) and SNAP-25A of the stabilized Q-SNARE complex were labeled with Oregon Green and Texas Red, respectively (see "Experimental Procedures" for details). The reaction was initiated by adding 40 nM labeled Syb(1–96) to liposomes containing labeled SNAP-25A. α-SNAP retarded SNARE assembly kinetics in a dose-dependent manner. *b* and *c*, membrane attachment of α-SNAP is critical for retardation of SNARE assembly. SNARE complex was not incorporated in liposomes (*b*). *d* and *e*, as an alternative assay, SNARE assembly was also monitored by following dissociation of the stabilizing synaptobrevin-2 peptide (*Syb(49–96)*) using fluorescence anisotropy. Syb(49–96) in the stabilized Q-SNARE complex was labeled with Alexa Fluor 488 (Syb(49–96)^{A488}) and incorporated in liposomes. The liposomes were preincubated for 5 min with WT α-SNAP (*d*) or α-SNAP (F27S, F28S) (*e*), followed by the addition of 50 nM unlabeled Syb(1–96) to monitor peptide dissociation as a read-out for SNARE complex formation. *f–h*, the mutants α-SNAP (F27S, F28S) and α-SNAP(33–295) differ in their ability to bind and disassemble membrane-anchored SNARE complexes. Binding of the α-SNAP variants was monitored by fluorescence anisotropy using either the soluble stabilized Q-SNARE complexes (consisting syntaxin-1A(183–262), SNAP-25A, and Syb(49–96)) (*f*) or membrane-anchored ternary complexes on CGs (endogenous synaptobrevin-2 displaces Syb(49–96)) (*g*), where syntaxin-1A was labeled at position Cys^{225} with Alexa Fluor 488. Note that under both conditions binding of WT α-SNAP and α-SNAP (F27S, F28S) was observed, whereas α-SNAP(33–295) did not bind. *h*, disassembly was monitored by FRET using membrane-anchored complexes as in *a*, in which Syb(1–96) and SNAP-25A of the stabilized Q-SNARE complex were labeled with Oregon Green and Texas Red, respectively. Dissociation was monitored by an increase in donor fluorescence due to the dissociation of SNAP-25A from the complex. 100 nM NSF and 5 mM ATP were included in buffer and 5 mM $MgCl_2$ was added to activate disassembly (*arrow*). The concentration of the α-SNAP variants (*f–h*) was 500 nM.

stabilized Q-SNARE complex as synaptobrevin-2 zippers in the N- to C-terminal direction (4). Using liposomes with a stabilized Q-SNARE complex containing Alexa 488-labeled Syb(49–96) (Syb(49–96)^{A488}), fragment displacement can be monitored by a decrease in fluorescence anisotropy as a result of enhanced fluorophore rotational mobility (4, 23, 26). We found that addition of soluble synaptobrevin-2 (Syb(1–96)) to acceptor liposomes resulted in rapid displacement of Syb(49–96)^{A488} in agreement with a previous observation (4), but was slowed down in the presence of α-SNAP (Fig. 4*d*). In contrast, both α-SNAP mutants in which the hydrophobic loop is perturbed or removed were unable to slow down displacement of Syb(49–96)^{A488} (Fig. 4*e*).

Interestingly, we found that the two α-SNAP mutants differ in their ability to bind to SNARE complexes. When binding was monitored using fluorescence anisotropy, we observed that

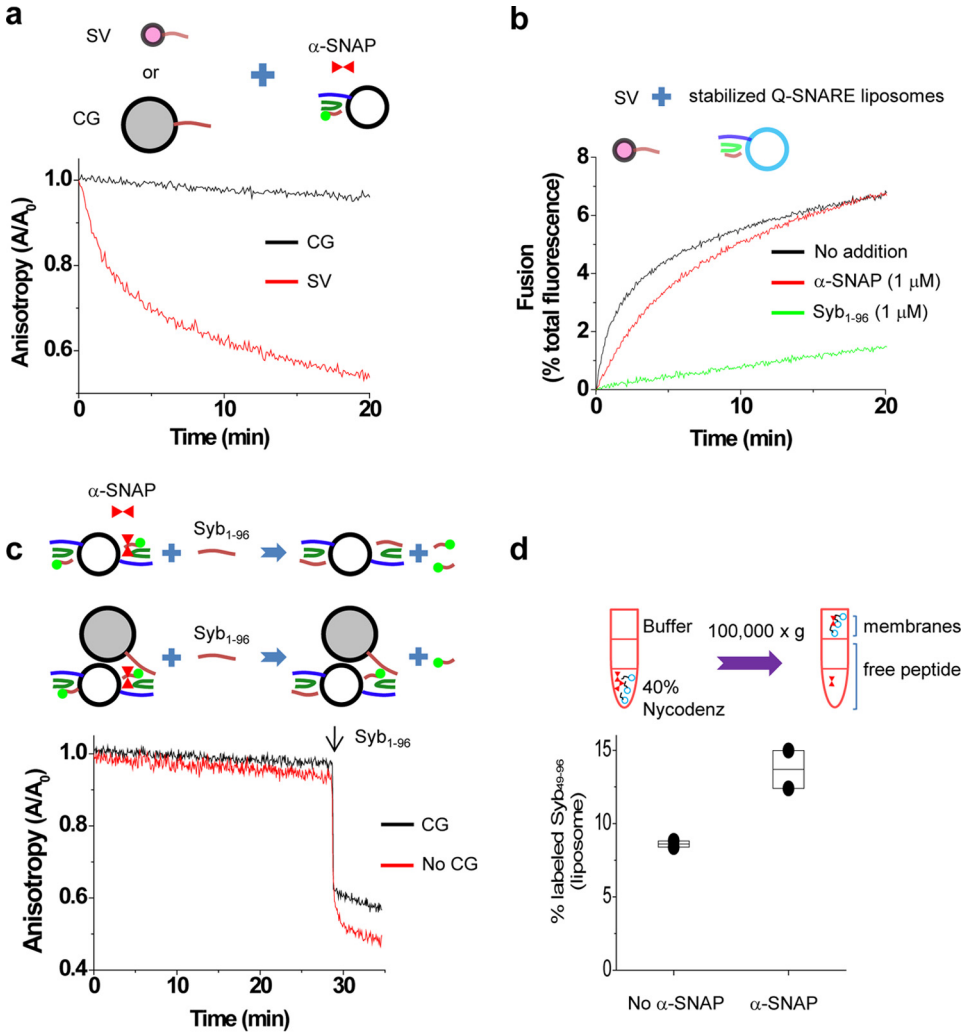

FIGURE 5. ***α*-SNAP arrests SNARE zippering midway.** *a*, displacement of the C-terminal peptide (Syb(49–96)^{A488}) from the stabilized acceptor complex is monitored by fluorescence anisotropy during SNARE assembly in the presence of 500 nM α-SNAP (see Fig. 5, *d* and *e*). *a*, effective peptide displacement was only seen upon fusion with SVs. *b*, displacement correlates with fusion between SVs and liposomes that was only slightly inhibited in the presence of α-SNAP. *c* and *d*, α-SNAP arrests SNARE zippering upstream of the peptide binding site. Acceptor liposomes containing labeled peptide (Syb(49–96)^{A488}) were incubated with α-SNAP either in the presence (docking) or absence of CGs. After 30 min, an excess of 1 μM unlabeled Syb(1–96) was added to displace all peptide from accessible SNARE complexes (see schematic). *c*, a pool of peptide was uncovered that could not be displaced when the liposomes were preincubated with CGs. *d*, synaptobrevin-2-containing liposomes were incubated with stabilized Q-SNARE acceptor liposomes in the presence (docking arrest) or absence (fusion) of α-SNAP, followed by addition of excess unlabeled Syb(1–96) as in *c*. The samples were then loaded on 40% Nycodenz media, overlaid with solution containing 30% Nycodenz followed by a layer of buffer and then centrifuged to separate membranes from free peptide by flotation. When α-SNAP was present, the amount of peptide retained on the membrane was higher. Non-displaced Syb(49–96)^{A488} in liposomes was presented as percentage of total Syb(49–96)^{A488} (two independent experiments). Note that the presence of peptide in the uninhibited reaction is due to the presence of inside-out oriented complexes that form during reconstitution and are not accessible to soluble Syb(1–96).

α-SNAP (F27S, F28S) bound to SNAREs with an efficiency comparable with that of α-SNAP (WT), whereas no binding was observed with α-SNAP(33–295), regardless of whether the soluble Q-SNAREs (Fig. 4*f*) or membrane-anchored ternary SNARE complexes (Fig. 4*g*) were used. Despite comparable binding, however, α-SNAP (F27S, F28S) was less efficient in NSF-driven disassembly of membrane-anchored SNARE complexes than α-SNAP (WT), whereas no disassembly was observed with α-SNAP(33–295) (Fig. 4*h*), in agreement with previous results (13). These findings suggest that binding as such has no effect on fusion, supporting the view that interference with SNARE zippering is due to a specific interaction involving the hydrophobic loop of α-SNAP with membranes.

Interference with SNARE Zippering in SVs and CGs by α-SNAP—In the final set of experiments, we tried to address at which stage zippering is affected by α-SNAP in reactions with CGs. As a point of comparison and in an attempt to obtain more generalized conclusions concerning trafficking vesicles, we decided to include SVs in our investigation. To this end, we again used the stabilized Q-SNARE complex with Syb(49–96)^{A488} and compared fragment displacement with CGs and SVs. We have shown previously that full zippering, measured by peptide displacement can occur, whereas fusion is blocked and SNAREs are assembled in *trans* (26), thus showing that peptide displacement can be used as a read-out for the degree of zippering. In the presence of α-SNAP, we observed virtually no displacement on reactions involving CGs (Fig. 5*a*). In contrast,

displacement of the Syb(49–96)^{A488} fragment was observed when SVs instead of CGs were used (Fig. 5*a*). We therefore checked whether α-SNAP interferes with fusion between SVs and liposomes and found that, in contrast to CGs, fusion was only slightly inhibited in the presence of α-SNAP (Fig. 5*b*). Together with all our previous analysis, these observations suggest that α-SNAP acts as a brake in the zippering reaction following the initiation of the *trans*-interaction. However, this retardation does not always seem to result in fusion being inhibited as revealed by the findings on SVs.

Although these results indicate that fusion inhibition originates from the interference of zippering as monitored by FRET assay (Fig. 4*a*) and peptide displacement (Fig. 4*d*), it is important to exclude a situation where docking is arrested but full zippering (and thereby peptide displacement) still occurs. Even though the strong retardation on displacement on CGs argues against this scenario (Fig. 5*a*), it could be that a very small fraction of peptides is displaced from *trans*-complexes and remains undetectable against the high background of unbound Q-SNARE complexes. Therefore, we added saturating amounts of unlabeled Syb(1–96) at the end of the reaction to drive off any Syb(49–96)^{A488} from unreacted Q-SNARE complexes, thus uncovering any bound peptides from *trans*-SNARE complexes that were assembled only partially. We found that anisotropy of Syb(49–96)^{A488} was higher in the presence of CGs and α-SNAP, indicating a fraction of the peptide could not be displaced by unlabeled Syb(1–96). This strongly indicates the presence of complexes with a "protected" nucleation site on the outer surface of the liposomes (Fig. 5*c*), supporting the idea that the docking arrest by α-SNAP is largely the result of partial and not fully zippered *trans*-SNARE complexes.

To further confirm the retention of the Syb(49–96)^{A488} fragment in the presence of α-SNAP, we separated displaced Syb(49–96)^{A488} from Q-SNARE complex-bound Syb(49–96)^{A488} using a density flotation gradient (Fig. 5*d*), revealing that a small but distinguishable amount of Syb(49–96)^{A488} remained bound to the Q-SNARE complex. Recalling that CGs and acceptor liposomes are kinetically trapped in a docked state in the presence of α-SNAP (Fig. 2), this finding further supports that at least some of the *trans*-SNARE complexes are only partially zippered.

DISCUSSION

In this study, we show that α-SNAP not only binds to Q-SNARE complexes but also interferes with zippering during SNARE complex formation. In large vesicles such as CGs (approximately 200 nm in diameter) this interference results in an arrest at a step prior to fusion during docking, a behavior that we could further demonstrate with SNARE-containing liposomes. Thus, our data provide a framework for rationalizing previous inhibitory effects of α-SNAP in the exocytosis of dense-core vesicles (100~300 nm in diameter) in PC12 cells (21), in yeast vacuoles (≤5 μm in diameter) (19, 20), and in acrosomal fusion (2~5 μm in diameter) (17, 18) following capacitation of sperm. In contrast, no effect of α-SNAP was observed when SVs were used, an observation that agrees well with a previous *in vivo* study reporting no significant inhibitory effect on exocytosis of SVs (31).

How exactly does α-SNAP interfere with SNARE zippering? α-SNAP is known to bind to the middle of the SNARE complex, raising the possibility that zippering of the central portion of the SNARE complex is mostly affected by α-SNAP (11). Indeed, the fact that the C-terminal fragment of synaptobrevin-2 (Syb(49–96)) is not displaced supports the view that zippering is arrested midway. We have previously demonstrated that mutations at the C-terminal end of synaptobrevin-2 can arrest a docked intermediate (26). However, here our biochemical characterization suggests that this can also be achieved by interfering with zippering further upstream of this region. Interestingly, many authors propose that such midway arrest is exactly the state of SNAREs in a docked and primed vesicle although the proteins proposed to cause such an arrest are different (complexin and synaptotagmin-1). Indeed, several lines of evidence involving CGs and direct force measurements of SNARE complex unzipping suggest the presence of an energy barrier in the middle of the SNARE complex (5, 32, 33). Thus, it is attractive to assume that such an energy barrier is enhanced by binding of α-SNAP. However, it needs to be borne in mind that the presence of Syb(49–96) used here as a reporter of zippering also contributes to the overall energy barrier and so the inhibitory effect might be more accentuated in the experimental conditions we investigated. Nevertheless, it is important to remember that inhibition was also seen when a Q-SNARE complex without stabilization by Syb(49–96) was used.

Although we have revealed that the binding of α-SNAP to the SNARE complex results in interference with zippering (Fig. 4*a*), this effect is not sufficiently strong to block progression to fusion under all circumstances as shown by our results on SVs (Fig. 5*b*). Rather, additional factors such as the properties of the membrane (*i.e.* SNARE density, curvature, protein and/or phospholipid composition) are likely involved in determining to which extent zippering interference by α-SNAP results in an inhibition of fusion. We have reported an analogous behavior with synaptobrevin-2 Δ84 containing a deletion that abrogates the +8 layer of the SNARE complex (26). In this case, the arrest is only observed with large (100 nm) liposomes but not between two small (40 nm) liposomes, a result we have rationalized in terms of their high curvature stress (26). Likewise, it is possible that SVs are inherently more fusogenic than CGs due to differences in curvature and lipid composition, providing an explanation as to why even though α-SNAP may still interfere with zippering in SVs, the transmitted force would still suffice for membrane merger. Further work will be required to conclusively test this hypothesis both *in vitro* and *in vivo*, but our findings lend strong support for a previously unnoticed SNARE zippering interference mechanism that inhibits fusion of CGs and large liposomes.

REFERENCES

1. Jahn, R., and Scheller, R. H. (2006) SNAREs: engines for membrane fusion. *Nat. Rev. Mol. Cell Biol.* **7,** 631–643
2. Martens, S., and McMahon, H. T. (2008) Mechanisms of membrane fusion: disparate players and common principles. *Nat. Rev. Mol. Cell Biol.* **9,** 543–556
3. Fasshauer, D., and Margittai, M. (2004) A transient N-terminal interaction of SNAP-25 and syntaxin nucleates SNARE assembly. *J. Biol. Chem.* **279,** 7613–7621

4. Pobbati, A. V., Stein, A., and Fasshauer, D. (2006) N- to C-terminal SNARE complex assembly promotes rapid membrane fusion. *Science* **313,** 673–676
5. Sørensen, J. B., Wiederhold, K., Müller, E. M., Milosevic, I., Nagy, G., de Groot, B. L., Grubmüller, H., and Fasshauer, D. (2006) Sequential N- to C-terminal SNARE complex assembly drives priming and fusion of secretory vesicles. *EMBO J.* **25,** 955–966
6. Li, F., Pincet, F., Perez, E., Eng, W. S., Melia, T. J., Rothman, J. E., and Tareste, D. (2007) Energetics and dynamics of SNAREpin folding across lipid bilayers. *Nat. Struct. Mol. Biol.* **14,** 890–896
7. Söllner, T., Bennett, M. K., Whiteheart, S. W., Scheller, R. H., and Rothman, J. E. (1993) A protein assembly-disassembly pathway in vitro that may correspond to sequential steps of synaptic vesicle docking, activation, and fusion. *Cell* **75,** 409–418
8. Clary, D. O., Griff, I. C., and Rothman, J. E. (1990) SNAPs, a family of NSF attachment proteins involved in intracellular membrane fusion in animals and yeast. *Cell* **61,** 709–721
9. Clary, D. O., and Rothman, J. E. (1990) Purification of three related peripheral membrane proteins needed for vesicular transport. *J. Biol. Chem.* **265,** 10109–10117
10. Wimmer, C., Hohl, T. M., Hughes, C. A., Müller, S. A., Söllner, T. H., Engel, A., and Rothman, J. E. (2001) Molecular mass, stoichiometry, and assembly of 20 S particles. *J. Biol. Chem.* **276,** 29091–29097
11. Marz, K. E., Lauer, J. M., and Hanson, P. I. (2003) Defining the SNARE complex binding surface of α-SNAP: implications for SNARE complex disassembly. *J. Biol. Chem.* **278,** 27000–27008
12. Chang, L. F., Chen, S., Liu, C. C., Pan, X., Jiang, J., Bai, X. C., Xie, X., Wang, H. W., and Sui, S. F. (2012) Structural characterization of full-length NSF and 20S particles. *Nat. Struct. Mol. Biol.* **19,** 268–275
13. Winter, U., Chen, X., and Fasshauer, D. (2009) A conserved membrane attachment site in α-SNAP facilitates *N*-ethylmaleimide-sensitive factor (NSF)-driven SNARE complex disassembly. *J. Biol. Chem.* **284,** 31817–31826
14. Hayashi, T., Yamasaki, S., Nauenburg, S., Binz, T., and Niemann, H. (1995) Disassembly of the reconstituted synaptic vesicle membrane fusion complex *in vitro*. *EMBO J.* **14,** 2317–2325
15. Hanson, P. I., Otto, H., Barton, N., and Jahn, R. (1995) The *N*-ethylmaleimide-sensitive fusion protein and α-SNAP induce a conformational change in syntaxin. *J. Biol. Chem.* **270,** 16955–16961
16. Babcock, M., Macleod, G. T., Leither, J., and Pallanck, L. (2004) Genetic analysis of soluble *N*-ethylmaleimide-sensitive factor attachment protein function in *Drosophila* reveals positive and negative secretory roles. *J. Neurosci.* **24,** 3964–3973
17. Tomes, C. N., De Blas, G. A., Michaut, M. A., Farré, E. V., Cherhitin, O., Visconti, P. E., and Mayorga, L. S. (2005) α-SNAP and NSF are required in a priming step during the human sperm acrosome reaction. *Mol. Hum. Reprod.* **11,** 43–51
18. Rodríguez, F., Bustos, M. A., Zanetti, M. N., Ruete, M. C., Mayorga, L. S., and Tomes, C. N. (2011) α-SNAP prevents docking of the acrosome during sperm exocytosis because it sequesters monomeric syntaxin. *PLoS One* **6,** e21925
19. Wang, L., Ungermann, C., and Wickner, W. (2000) The docking of primed vacuoles can be reversibly arrested by excess Sec17p (α-SNAP). *J. Biol. Chem.* **275,** 22862–22867
20. Mayer, A., Wickner, W., and Haas, A. (1996) Sec18p (NSF)-driven release of Sec17p (α-SNAP) can precede docking and fusion of yeast vacuoles. *Cell* **85,** 83–94
21. Barszczewski, M., Chua, J. J., Stein, A., Winter, U., Heintzmann, R., Zilly, F. E., Fasshauer, D., Lang, T., and Jahn, R. (2008) A novel site of action for α-SNAP in the SNARE conformational cycle controlling membrane fusion. *Mol. Biol. Cell* **19,** 776–784
22. Collins, K. M., and Wickner, W. T. (2007) Trans-SNARE complex assembly and yeast vacuole membrane fusion. *Proc. Natl. Acad. Sci. U.S.A.* **104,** 8755–8760
23. Park, Y., Hernandez, J. M., van den Bogaart, G., Ahmed, S., Holt, M., Riedel, D., and Jahn, R. (2012) Controlling synaptotagmin activity by electrostatic screening. *Nat. Struct. Mol. Biol.* **19,** 991–997
24. Takamori, S., Holt, M., Stenius, K., Lemke, E. A., Grønborg, M., Riedel, D., Urlaub, H., Schenck, S., Brügger, B., Ringler, P., Müller, S. A., Rammner, B., Gräter, F., Hub, J. S., De Groot, B. L., Mieskes, G., Moriyama, Y., Klingauf, J., Grubmüller, H., Heuser, J., Wieland, F., and Jahn, R. (2006) Molecular anatomy of a trafficking organelle. *Cell* **127,** 831–846
25. Weber, T., Zemelman, B. V., McNew, J. A., Westermann, B., Gmachl, M., Parlati, F., Söllner, T. H., and Rothman, J. E. (1998) SNAREpins: minimal machinery for membrane fusion. *Cell* **92,** 759–772
26. Hernandez, J. M., Stein, A., Behrmann, E., Riedel, D., Cypionka, A., Farsi, Z., Walla, P. J., Raunser, S., and Jahn, R. (2012) Membrane fusion intermediates via directional and full assembly of the SNARE complex. *Science* **336,** 1581–1584
27. Cypionka, A., Stein, A., Hernandez, J. M., Hippchen, H., Jahn, R., and Walla, P. J. (2009) Discrimination between docking and fusion of liposomes reconstituted with neuronal SNARE-proteins using FCS. *Proc. Natl. Acad. Sci. U.S.A.* **106,** 18575–18580
28. Müller, C. B., Loman, A., Richtering, W., and Enderlein, J. (2008) Dual-focus fluorescence correlation spectroscopy of colloidal solutions: influence of particle size. *J. Phys. Chem. B* **112,** 8236–8240
29. Hayashi, T., McMahon, H., Yamasaki, S., Binz, T., Hata, Y., Südhof, T. C., and Niemann, H. (1994) Synaptic vesicle membrane fusion complex: action of clostridial neurotoxins on assembly. *EMBO J.* **13,** 5051–5061
30. Siddiqui, T. J., Vites, O., Stein, A., Heintzmann, R., Jahn, R., and Fasshauer, D. (2007) Determinants of synaptobrevin regulation in membranes. *Mol. Biol. Cell* **18,** 2037–2046
31. Burgalossi, A., Jung, S., Meyer, G., Jockusch, W. J., Jahn, O., Taschenberger, H., O'Connor, V. M., Nishiki, T., Takahashi, M., Brose, N., and Rhee, J. S. (2010) SNARE protein recycling by αSNAP and βSNAP supports synaptic vesicle priming. *Neuron* **68,** 473–487
32. Gao, Y., Zorman, S., Gundersen, G., Xi, Z., Ma, L., Sirinakis, G., Rothman, J. E., and Zhang, Y. (2012) Single reconstituted neuronal SNARE complexes zipper in three distinct stages. *Science* **337,** 1340–1343
33. Min, D., Kim, K., Hyeon, C., Cho, Y. H., Shin, Y. K., and Yoon, T. Y. (2013) Mechanical unzipping and rezipping of a single SNARE complex reveals hysteresis as a force-generating mechanism. *Nat. Commun.* **4,** 1705